Original Article

Diagnostic accuracy of contrast-enhanced ultrasound synchronized with shear wave elastography in the differential diagnosis of benign and malignant breast lesions: a diagnostic test

Huiling He[1#^], Xiaojin Wu[2#^], Meijuan Jiang[2^], Zhikang Xu[2^], Xuanxuan Zhang[1^], Jianlian Pan[3^], Xinyu Fu[1^], Yunkai Luo[1^], Jian Chen[1^]

[1]Department of Ultrasound Medicine, the Fourth Affiliated Hospital of Zhejiang University School of Medicine, Yiwu, China; [2]Zhejiang University School of Medicine, Hangzhou, China; [3]Department of Clinical and Research, Shenzhen Mindray Bio-Medical Electronics Co., Ltd., Shenzhen, China

Contributions: (I) Conception and design: H He, X Wu, M Jiang, J Chen, J Pan; (II) Administrative support: J Chen; (III) Provision of study materials or patients: H He, X Wu, M Jiang, Y Luo; (IV) Collection and assembly of data: H He, X Wu, Z Xu, X Zhang; (V) Data analysis and interpretation: X Wu, X Fu; (VI) Manuscript writing: All authors; (VII) Final approval of manuscript: All authors.

[#]These authors contributed equally to this work.

Correspondence to: Jian Chen. Department of Ultrasound Medicine, the Fourth Affiliated Hospital of Zhejiang University School of Medicine, 1 Shang Cheng Avenue, Yiwu 322000, China. Email: chenjianzuj4h@zju.edu.cn.

Background: Breast cancer (BC) is one of the most common malignancies affecting women. Timely and accurate diagnosis is crucial for treatment and prognosis. Some studies have found that elastography combined with microperfusion characteristics, which are mostly described by contrast-enhanced ultrasound (CEUS), could help in the diagnosis of breast lesions. This study aimed to assess the diagnostic performance of CEUS synchronized with shear wave elastography (SWE) in discriminating between benign and malignant breast lesions by using real-time contrast elastography images to analyze shell elasticity and contrast intensity.

Methods: A total of 26 pathologically confirmed breast lesions in 26 patients were retrospectively reviewed. Each patient underwent conventional B-mode ultrasound, CEUS, and then SWE data was obtained from a frame of image that was almost identical to the B-mode and CEUS images when acquiring time to peak (TTP). Breast lesions were evaluated based on the Breast Imaging Reporting and Data System (BI-RADS) and quantitative characteristics that describe the stiffness and intensity of contrast of the 1.0–3.0 mm shell region. Quantitative aspects of the inner lesions and shell on the elastogram included the maximum (Emax), mean (Emean), and minimum (Emin) Young's moduli. Quantitative enhanced features included maximum (Imax) and mean (Imean) intensity. We took postoperative pathological results as the gold standard. Receiver operating characteristic (ROC) curves were used to compare the diagnostic efficacy of the 2 examination modalities, either alone or in combination.

Results: The age of the patients ranged from 23 to 76 years, with a 42.5-year average age. In all breast lesions, 19 were benign and 7 were malignant. SWE synchronized with CEUS can effectively improve the diagnostic performance of breast lesions, and Emean + Imean and Emax + Emean + Imean of shell at 1.0 mm both had the highest area under the curve (AUC) of 0.86 [95% confidence interval (CI): 0.67, 0.96], with the

^ ORCID: Huiling He, 0000-0002-3404-3506; Xiaojin Wu, 0000-0001-7469-4429; Meijuan Jiang, 0000-0003-3037-3791; Zhikang Xu, 0000-0001-9385-3317; Xuanxuan Zhang, 0000-0001-6797-3489; Jianlian Pan, 0000-0002-5829-4641; Xinyu Fu, 0000-0001-5895-5238; Yunkai Luo, 0000-0001-9081-5577; Jian Chen, 0000-0003-2295-5505.

sensitivity and specificity of 71.43% and 89.47%, respectively.

Conclusions: The combination of CEUS and SWE has a better diagnostic value in differentiating benign and malignant breast lesions compared to separate techniques.

Keywords: Breast; contrast-enhanced ultrasound (CEUS); shear wave elastography (SWE); ultrasonography (US)

Submitted Oct 20, 2022. Accepted for publication Jan 06, 2023. Published online Jan 13, 2023.
doi: 10.21037/gs-22-684
View this article at: https://dx.doi.org/10.21037/gs-22-684

Introduction

Breast cancer (BC) is one of the most prevalent malignancies affecting women. According to the Global Cancer Statistics 2020, BC has surpassed lung cancer as the leading cause of global cancer in 2020 (1). In China, BC has the highest morbidity and mortality among female malignancies (2). Therefore, timely and accurate diagnosis is crucial for treatment and prognosis (3). An essential tool for detecting breast lesions is breast ultrasonography (US), which is cheap, convenient, non-radiative, and offers real-time results. The standardized Breast Imaging Reporting and Data System (BI-RADS) Classification System (4) has been used to evaluate the risk of breast lesions.

However, the incidence of BC is highly variable, which might result in unnecessary biopsies. Non-invasive elastography has been proposed as a means to improve differentiation between benign and malignant breast lesions. Through the use of focused ultrasonic beams, the technique induces mechanical vibrations in tissue and measures its stiffness through the detection of propagating shear waves (5). In several studies, shear wave elastography (SWE) combined with US has been found to perform well in the differentiation process (6,7). Cui *et al.* (8) found that the hardest areas of breast lesions were at the periphery rather than the interior, and the diagnostic value of maximum elastic (Emax) when the thickness of stiff rim which also known as shell was at 2.0 mm was the highest [area under the curve (AUC) =0.930] with a sensitivity of 87.5% and specificity of 88%, which means that elasticity analysis at the periphery may be useful for diagnosis, accordingly.

Studies have shown that BC is highly correlated with microvessel angiogenesis (9,10), which is very important to the growth, invasion, and survival of breast lesions. Furthermore, compared with benign lesions, malignant lesions have displayed a significantly different microvascular architecture (11). However, color Doppler flow imaging (CDFI) has only been used to evaluate vessels up to 0.2 mm in diameter (12), due to which it has been shown to be less discriminative than other invasive methods, such as contrast-enhanced ultrasound (CEUS) and contrast-enhanced magnetic resonance image (CE-MRI). In some studies, CEUS has been shown to provide information on microperfusion in benign and malignant BC (13). Cancerous tissues become harder as the blood vessel and cell density increase, and stiffness is associated with tumor progression (14).

Studies have revealed that elastography combined with blood flow characteristics could also help to enhance the diagnostic performance in identifying malignant and benign breast lesions (15,16). To our best knowledge, there have been no studies on CEUS in the assessment of microvascular characteristics in the peripheral regions of breast lesions, so as to differentiate between benign

Highlight box

Key findings

- The combined use of CEUS and SWE in the peripheral region has a better diagnostic value in differentiating benign and malignant breast lesions compared to separate techniques.

What is known and what is new?

- Elastography combined with microperfusion characteristics, which are mostly described by CEUS, could help in the diagnosis of breast lesions.
- This study aimed to assess the diagnostic performance of CEUS synchronized with SWE in discriminating between benign and malignant breast lesions by using real-time contrast elastography images to analyze shell elasticity and contrast intensity.

What is the implication, and what should change now?

- In identifying benign and malignant breast lesions, it is possible to identify them not only by the parameter of stiffness around the lesion, but also by the parameter of contrast intensity around the lesion, which is a brand-new direction of research, to our knowledge.

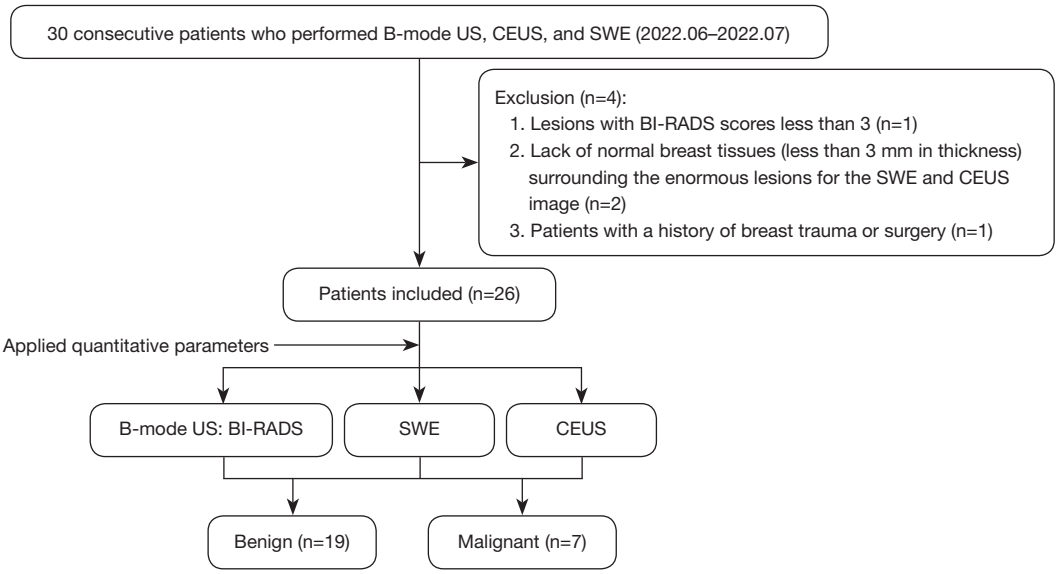

Figure 1 Flowchart illustrating the study process. US, ultrasound; CEUS, contrast-enhanced ultrasound; SWE, shear wave elastography; BI-RADS, Breast Imaging Reporting and Data System.

and malignant breast lesions. The aim of this study was to evaluate the diagnostic efficiency of SWE, CEUS, and SWE synchronized with CEUS for distinguishing between benign and malignant breast lesions, with special emphasis on the value of the peripheral tissue. We present the following article in accordance with the STARD reporting checklist (available at https://gs.amegroups.com/article/view/10.21037/gs-22-684/rc).

Methods

Patients

The included patients' ages ranged from 23 to 76, with a 42.5-year average age, and the lesions' maximum diameters ranged from 6.10 to 38.70 mm. Before examination, all patients provided written informed consent to undergo CEUS. From June 2022 to July 2022, conventional US, CEUS, and SWE were performed on 30 women with 30 breast lesions, who planned a surgery of breast lesions.

The inclusion criteria were as follows: (I) breast lesions palpable by an oncologist or could be observed on the conventional ultrasound (US); (II) no hospitalization, radiotherapy, or chemotherapy was performed for BC before enrollment.

The exclusion criteria were as follows: (I) lesions with BI-RADS values under 3 as determined by traditional US techniques; (II) lack of normal breast tissues (less than 3 mm in thickness) around the gross lesions for the SWE and CEUS image; (III) patients who have had breast surgery or trauma in the past.

Only lesions with the highest BI-RADS category were evaluated. When several lesions were classified in the same BI-RADS category, the lesion with the largest diameter was included. *Figure 1* displays a flowchart illustrating the study process. The study was conducted in accordance with the Declaration of Helsinki (as revised in 2013). The study was approved by Ethics Committee of the Fourth Affiliated Hospital of Zhejiang University School of Medicine (No. K2022168) and individual consent for this retrospective analysis was waived.

Ultrasound equipment

The Conventional US, CEUS, and SWE were obtained by using a Resona 9 diagnostic US system (Mindray Medical International, Shenzhen, China). The probe used for Conventional US and SWE was 3–15 MHz. The probe used for CEUS was 3–11 MHz. The contrast agent used was SonoVue (Bracco, Italy). There was a unique toolbox included with the diagnostic system for shell quantification, which was applied to measure the stiffness and peak intensity (PKI) of the margin (0.5–9 mm), around which was measured in increments of 0.5 mm.

Image acquisition

Conventional US, CEUS, and SWE examinations were performed by the same radiologist (HLH) with 10 years of experience in breast US, who did not know the pathological diagnosis of the breast lesions. The patients were required to remain supine with the breast and axilla fully exposed. First, a typical gray-scale section was detected, and the transverse and longitudinal US images of the lesions were obtained. All conventional US aspects of the lesions, including size, shape, edge, location, echo pattern, calcification, and related features, were evaluated based on the conventional US images. Then, the final BI-RADS assessment category was determined. According to the BI-RADS categories: BI-RADS 3, ultrasound of the breast revealed a likely benign feature; BI-RADS 4a, 4b, and 4c were classified as low, medium, and high malignant suspicion, respectively; BI-RADS 5 was highly indicative of malignancy. According to the guidelines of the American Society of Radiology, a biopsy was advised for breast lesions with BI-RADS 4a or higher.

The following actions were taken in order to obtain CEUS images. To begin the CEUS, the cut surface with the most robust blood flow and well-defined vascularity of the lesion was chosen. A 4.8 mL bolus of the US contrast agent was intravenously given, and then it was flushed with a 5.0 mL solution of 0.9% sodium chloride (17). As soon as the timer began, a continuous video recording (for at least 2 minutes) was made, and pictures and videos were saved for analysis. The patients were told to breathe slowly and steadily during acquisition, and the operator positioned the probe lightly on the skin in front of the lesion to prevent excessive pressure from impairing the contrast agent microvascular imaging. The acquired videos were further processed with analysis software. In order to obtain the corresponding time and image of PKI, the radiologist drew a region of interest (ROI) by tracing the margin of the lesions. The time-intensity curve (TIC) was recorded automatically, and the quantitative parameters were generated, including PKI and time to peak (TTP). After obtaining the TTP, the radiologist advanced the video to the corresponding frame to obtain both B-mode and CEUS images of the lesions. In order to obtain the elasticity images correctly, the following steps were performed. Following the previous images, the transducer was placed vertically and as lightly as possible on the surface above the lesion. The patient was instructed to breathe slowly and steadily during the entire session. Meanwhile, a rectangular ROI was set to obtain SWE images, which should have included the entire breast lesion and any adjacent tissue no less than 3 mm. The dependability of the SWE images was evaluated through the use of the quality control parameter called similarity, which ranged from 0% to 100%. When similarity reached more than 90%, we assumed the current image was almost identical to the B-mode and CEUS image. Meanwhile, a shear wave quality mode was used to evaluate the accuracy of the SWE images: Chart for Quality Control (QCC). The SWE images were regarded as being of high quality when the color in the QCC was consistent. Once the image was stabilized and of high quality, the image was saved for further analysis, and the lesions' boundaries were manually delineated. The maximum, mean, and minimum Young's moduli (0–140 kPa) of the lesions could be calculated and documented as Emax, Emean, and Emin. The maximum and mean intensity values of the lesions could also be calculated and documented as Imax and Imean. By adjusting the "shell" function key to 1.0, 2.0, and 3.0 mm, the maximum elastic modulus, mean elastic modulus, minimum elastic modulus, maximum intensity, and mean intensity of the "shell" area were automatically calculated. Finally, the average of the data was calculated and included into the study (*Figures 2,3*).

Histopathological examination

Results from histopathology were regarded as the gold standard, which were carried out by a pathologist who specialized in disorders of the breast. The pathologist was blinded to the results of ultrasound.

Statistical analysis

The software SPSS 26.0 (IBM Corp., Armonk, NY, USA) was used to perform statistical analysis; the independent samples Kolmogorov-Smirnov was used to confirm the normal distribution. Continuous data satisfying the normal distribution are expressed as the mean ± standard deviation (SD), the independent samples *t*-test was used to compare the quantitative Young's moduli and intensity values. Receiver operating characteristic (ROC) curve analysis was performed by using MedCalc for Windows, version 20.0.22 (MedCalc Software Ltd., Ostend, Belgium). Optimal cutoff values were determined through the Youden index. The sensitivity, specificity, positive predictive values (PPVs), negative predictive values (NPVs), and AUC of CEUS, SWE, and the combination in the diagnosis of benign and

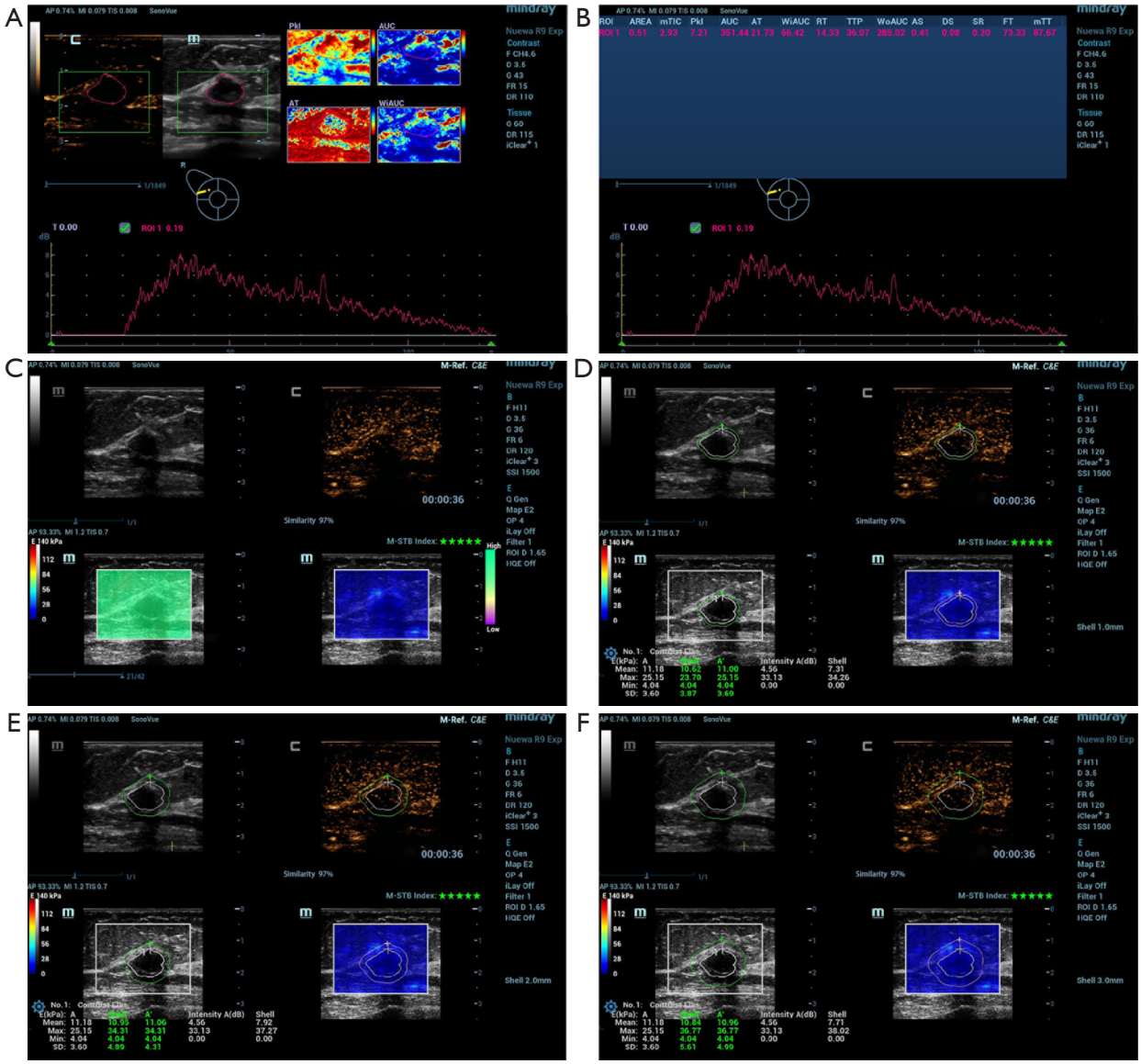

Figure 2 53-year-old woman with fibroadenoma. (A) ROI for quantitative analysis of CEUS. (B) Quantitative analysis of TIC of CEUS, which showed the TTP was 36.07 s. (C) CEUS synchronized with SWE quality control with no obvious artifacts. (D) The shell included 1.0 mm peripheral tissue surrounding the breast lesion. The values of Emax, Emean, Emin, Imax, and Imean were 23.70 kPa, 10.62 kPa, 4.04 kPa, 34.26 dB, and 7.31 dB, respectively. (E) The shell included 2.0 mm peripheral tissue surrounding the breast lesion. The values of Emax, Emean, Emin, Imax, and Imean were 34.31 kPa, 10.95 kPa, 4.04 kPa, 37.27 dB, and 7.92 dB, respectively. (F) The shell included 3.0 mm peripheral tissue surrounding the breast lesion. The values of Emax, Emean, Emin, Imax, and Imean were 36.77 kPa, 10.84 kPa, 4.04 kPa, 38.02 dB, and 7.71 dB, respectively. ROI, region of interest; CEUS, contrast-enhanced ultrasound; TIC, time-intensity curve; TTP, time to peak; SWE, shear wave elastography; Emax, the maximum Young's moduli; Emean, the mean Young's moduli; Emin, the minimum Young's moduli; Imax, the maximum intensity; Imean, the mean intensity.

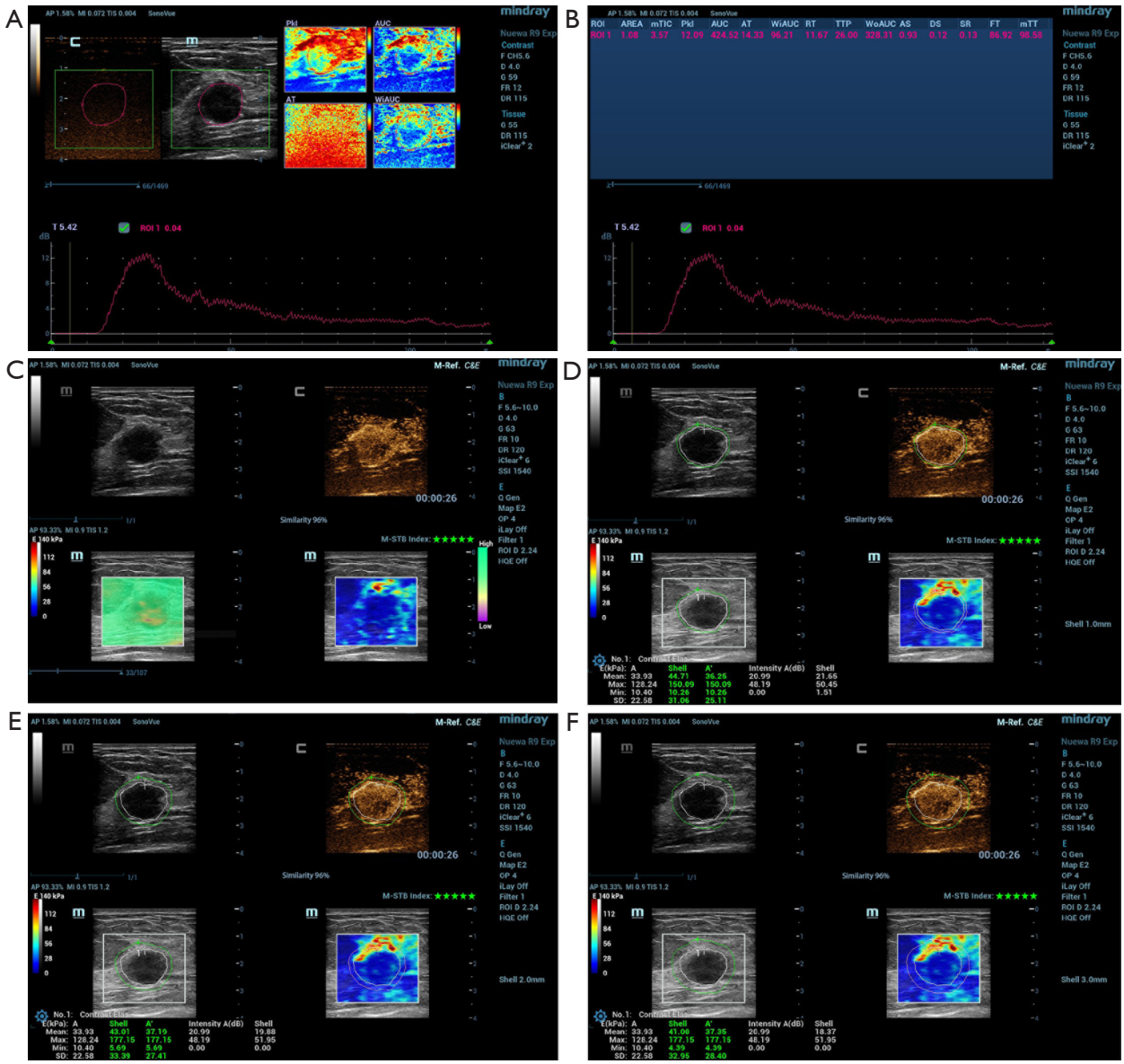

Figure 3 36-year-old woman with invasive lobular carcinoma. (A) ROI for quantitative analysis of CEUS. (B) Quantitative analysis of TIC of CEUS, which showed the TTP was 26.00 s. (C) CEUS synchronized with SWE quality control with no obvious artifacts. (D) The shell included 1.0 mm peripheral tissue surrounding the breast lesion. The values of Emax, Emean, Emin, Imax, and Imean were 150.09 kPa, 44.71 kPa, 10.26 kPa, 50.45 dB, and 21.65 dB, respectively. (E) The shell included 2.0 mm peripheral tissue surrounding the breast lesion. The values of Emax, Emean, Emin, Imax, and Imean were 177.15 kPa, 43.01 kPa, 5.69 kPa, 51.95 dB, and 19.88 dB, respectively. (F) The shell included 3.0 mm peripheral tissue surrounding the breast lesion. The values of Emax, Emean, Emin, Imax, and Imean were 177.15 kPa, 41.00 kPa, 4.39 kPa, 51.95 dB, and 18.37 dB, respectively. ROI, region of interest; CEUS, contrast-enhanced ultrasound; TIC, time-intensity curve; TTP, time to peak; SWE, shear wave elastography; Emax, the maximum Young's moduli; Emean, the mean Young's moduli; Emin, the minimum Young's moduli; Imax, the maximum intensity; Imean, the mean intensity.

Table 1 Histopathological results of benign and malignant breast lesions

Histopathological finding	No. of lesions (%)
Benign	
Fibroadenoma	12 (63.16)
Intraductal papilloma	5 (26.32)
Inflammation	1 (5.26)
Hyperplastic nodule	1 (5.26)
Malignant	
Invasive ductal carcinoma	3 (42.86)
Invasive lobular carcinoma	2 (28.57)
Ductal carcinoma in situ	2 (28.57)

malignant nodules were calculated, with postoperative pathological results as the gold standard. When the P value was less than 0.05, differences were declared statistically significant.

Results

Pathological findings

Out of 26 breast lesions, postoperative histology found 19 benign and 7 malignant lesions. The included patients' ages ranged from 23 to 76, with a 42.5-year average age. In our study, the average age of the benign and malignant patients was 41.16±13.50 years (range, 23–66 years) and 46.00±15.66 years (range, 30–76 years), respectively. The lesions' maximum diameters ranged from 6.10 to 38.70 mm, with benign and malignant lesions having mean diameters of 15.99±9.03 and 23.06±9.95 mm, respectively. Age and size differences between benign and malignant breast tumors were not found to be statistically significant (P>0.05). Histopathological results of the benign and malignant tumors are summarized in *Table 1*.

The characteristics of quantitative SWE

Emean of lesions, Emax and Emean of the shell at 1.0 mm, Emean of the shell at 2.0 mm, and Emean of the shell at 3.0 mm were higher in malignant breast lesions than benign lesions (P<0.05) (*Table 2*). Based on the ROC analysis, only Emean of shell at 3.0 mm, with an AUC of 0.74 [95% confidence interval (CI): 0.54, 0.89], presented significant difference between benign and malignant lesions. The sensitivity, specificity, PPV, and NPV are presented in *Table 3*.

The characteristics of quantitative CEUS

Regarding the CEUS image, the difference in Imax of lesions, Imean of the shell at 1.0 mm, and Imean of the shell at 2.0 mm between benign and malignant breast lesions were considerable. However, when the shell was at 3.0 mm, it did not appear that benign and malignant lesions differed much in terms of the intensity (*Table 4*). The AUCs of the Imax of lesions, Imean of the shell at 1.0 mm, and Imean of the shell at 2.0 mm were 0.74 (95% CI: 0.53, 0.89), 0.81 (95% CI: 0.61, 0.94), and 0.81 (95% CI: 0.60, 0.93), respectively. The Imean of the shell at 1.0 mm had the maximum AUC of 0.81. The sensitivity, specificity, PPV, and NPV are presented in *Table 3*.

Diagnostic performance when CEUS was synchronized with SWE

The AUCs of Emean + Imax of lesions, Emax + Imean of the shell at 1.0 mm, Emean + Imean of shell at 1.0 mm, Emax + Emean + Imean of shell at 1.0 mm, and Emean + Imean of shell at 2.0 mm were 0.77 (95% CI: 0.57, 0.91), 0.86 (95% CI: 0.67, 0.96), 0.85 (95% CI: 0.66, 0.96), 0.86 (95% CI: 0.67, 0.96), and 0.82 (95% CI: 0.62, 0.94), respectively (P<0.05 for all). The sensitivity, specificity, PPV, and NPV are presented in *Table 3*.

Discussion

The standard BI-RADS grading system is widely used to assess the risk assessment of breast lesions, which is mainly based on 2-dimensional (2D) grey-scale US (18). However, the scoring system is highly sensitive but less specific, which makes it difficult to distinguish between benign and malignant breast lesions. With the development of elastography and CEUS technology, radiologists can obtain both the conventional observation information, like morphology and blood flow characteristics of the lesion, and the stiffness in and around the lesion, which helps to improve the diagnostic accuracy (19).

A previous study has indicated that instead of the center of the lesions, the periphery of malignant breast lesions is the hardest (20). There has been increasing concern about the peripheral area of breast lesions, particularly the stiffness of the shell. According to certain researches, employing the shell-based analysis technique, Emax of the

Table 2 SWE results of benign and malignant breast lesions

Variable	Benign (n=19)	Malignant (n=7)	t value	P value
Lesion				
Emax (kPa)	61.55±30.14	135.18±108.88	−1.765	0.125
Emean (kPa)	22.40±7.60	31.13±13.68	−2.079	0.049
Emin (kPa)	8.00±3.24	7.64±3.61	0.252	0.803
Shell 1.0 mm				
Emax (kPa)	67.07±41.74	124.54±70.15	−2.581	0.016
Emean (kPa)	25.53±11.74	40.87±18.05	−2.551	0.018
Emin (kPa)	8.12±3.96	9.37±2.78	−0.759	0.456
Shell 2.0 mm				
Emax (kPa)	83.59±53.90	135.02±70.31	−1.991	0.058
Emean (kPa)	26.07±12.81	40.92±16.94	−2.406	0.024
Emin (kPa)	7.60±3.70	8.31±3.22	−0.445	0.660
Shell 3.0 mm				
Emax (kPa)	92.92±67.26	140.05±63.30	−1.608	0.121
Emean (kPa)	26.07±13.21	39.22±14.48	−2.196	0.038
Emin (kPa)	6.86±3.17	6.93±4.16	−0.041	0.967

The data are expressed as mean ± standard deviation. SWE, shear wave elastography; Emax, the maximum Young's moduli; Emean, the mean Young's moduli; Emin, the minimum Young's moduli.

shell at 1.0–3.0 mm demonstrated the highest diagnostic performance when differentiating between benign and malignant breast tumors (21-23). There are two main reasons which can explain this phenomenon. One is that the peritumoral stiffness is increased by the presence of abnormal stiff collagen associated with cancer fibroblasts and the desmoplastic reaction brought on by the invasion of cancer cells into the peri-lesions (20,24,25). The other is that the energy of shear waves is reduced in nearby regions, which leads to lower elastic values inside breast lesions (20,23). In our study, the elasticity of the shell at 1.0–3.0 mm could differentiate benign and malignant breast lesions, though only several parameters could distinguish with significant difference. This result is similar to previous studies, generally. Additionally, when it comes to the ROC curve of SWE, only Emean of the shell at 3.0 mm with an AUC at 0.74 (95% CI: 0.54, 0.89) was statistically different. This was mainly because our sample size was limited, which may have led to increased error. Meanwhile, invasive ductal carcinoma and ductal carcinoma in situ (DCIS) accounted for a large proportion, which have a minimal potential to invade the surrounding tissue. These may together result in Emean being statistically significant in differentiating between benign and malignant lesions.

The mammary gland is a superficial organ with a poor blood supply, which causes a slower blood flow (26). However, the conventional CDFI technique cannot visualize low velocity blood flows. CEUS is one of the recognized sensitive methods for BC detection. It provides microperfusion information by injecting a contrast agent, which forms contrast agent microbubbles at the air-liquid interface to enhance the Doppler signal of blood flow. Li *et al.* (27) analyzed the CEUS and histopathology of BC, and concluded that the CEUS and parameters of CEUS could not only reflect microvascular distribution, but also indirectly indicate the histological grade of BC. According to several investigations, peripheral rim enhancement on magnetic resonance imaging (MRI) has been linked to greater tumor size, higher histologic grade, estrogen receptor (ER)-negativity, progesterone receptor (PR)-negativity, and positive lymph node status (28,29). Few studies have examined the value of shell area enhancement characteristics in distinguishing benign and malignant breast masses, let alone the quantitative analysis of the shell

Table 3 Diagnostic performance of SWE, CEUS, and SWE + CEUS in distinguishing malignant from benign masses

Group	Variable	Sensitivity (%)	Specificity (%)	PPV (%)	NPV (%)	AUC (95% CI)	P value
SWE							
Lesion	Emean	71.43	78.95	55.53	88.24	0.72 (0.51–0.88)	0.125
Shell 1.0 mm	Emax	71.43	94.74	83.32	90.01	0.76 (0.55–0.90)	0.057
	Emean	71.43	89.47	71.39	89.48	0.74 (0.53–0.89)	0.067
Shell 2.0 mm	Emean	71.43	89.47	71.39	89.48	0.74 (0.53–0.89)	0.052
Shell 3.0 mm	Emean	71.43	89.47	71.40	89.48	0.74 (0.54–0.89)	0.044
CEUS							
Lesion	Imax	85.71	68.42	49.97	92.86	0.74 (0.53–0.89)	0.013
Shell 1.0 mm	Imean	85.71	73.68	54.51	93.34	0.81 (0.61–0.94)	0.002
Shell 2.0 mm	Imean	71.43	84.21	62.47	88.90	0.81 (0.60–0.93)	0.001
Shell 3.0 mm (NA)							
SWE + CEUS							
Lesion	Emean + Imax	71.43	78.95	55.53	88.25	0.77 (0.57–0.91)	0.016
Shell 1.0 mm	Emax + Imean	71.43	89.47	71.40	89.48	0.86 (0.67–0.96)	<0.001
	Emean + Imean	85.71	73.68	54.51	93.34	0.85 (0.66–0.96)	<0.001
	Emax + Emean + Imean	71.43	89.47	71.40	89.49	0.86 (0.67–0.96)	<0.001
Shell 2.0 mm	Emean + Imean	71.43	84.21	62.47	88.90	0.82 (0.62–0.94)	0.002
Shell 3.0 mm (NA)							

SWE, shear wave elastography; CEUS, contrast enhanced ultrasound; PPV, positive predictive value; NPV, negative predictive value; AUC, the area under the receiver operating characteristic curve; Emax, the maximum Young's moduli; Emean, the mean Young's moduli; Imean, mean intensity; Imax, maximum intensity; NA, not applicable.

region enhancement characteristics to assess benign and malignant characteristics.

We were able to retrieve only 2 articles on peripheral enhancement of BC, which both demonstrated that the peripheral enhancement pattern is suggestive of malignancy, with a diagnostic sensitivity, specificity, and accuracy of 39.5%, 98.3%, and 73.8%, respectively (11,30). However, these 2 studies used categorical variables; breast CEUS morphologic classification is subjective, and it might be challenging to distinguish between distinct enhancing patterns. This study, to the best of our knowledge, is the first to use quantitative analysis of shell enhancement and stiffness to distinguish benign and malignant breast tumors. The maximum intensity of lesion, mean intensity of shell at 1.0 mm, and mean intensity of shell at 2.0 mm are significantly higher in malignant breast lesions (P<0.05), which means peripheral enhancement is valuable in differentiating benign and malignant breast tumors. The AUCs of intensity parameters all showed significant difference (P<0.05). The AUCs of CEUS in shell region, which were 0.81 (95% CI: 0.61, 0.94), and 0.81 (95% CI: 0.60, 0.93) when the shell was 1.0 and 2.0 mm, were both larger than that of the lesion, which was 0.74 (95% CI: 0.53, 0.89). This result is consistent with previous studies on peripheral enhancement.

In our study, we also analyzed the ROI of SWE synchronized with CEUS. We selected the image corresponding to TTP, and used the similarity and QQC quality control parameters to obtain the best images for stiffness of shell region, which can avoid the shortcoming of poor correlation between elastic and enhancement results under different sections, to some extent. In conventional elastography and CEUS studies, researchers have typically chosen the largest diameter planes to measure elasticity and the most abundant Doppler signal planes to measure enhancement (31-33), which were 2 different images, in

Table 4 CEUS results of benign and malignant breast lesions

Variable	Benign	Malignant	t value	P value
Lesion				
Imax (dB)	46.32±10.87	52.06±2.64	−2.135	0.044
Imean (dB)	17.18±8.44	22.53±4.41	−1.585	0.126
Shell 1.0 mm				
Imax (dB)	44.80±10.08	50.99±3.28	−1.575	0.128
Imean (dB)	14.19±5.28	19.37±3.42	−2.402	0.024
Shell 2.0 mm				
Imax (dB)	47.67±8.98	51.47±3.69	−1.074	0.294
Imean (dB)	13.28±5.01	17.49±3.12	−2.065	0.050
Shell 3.0 mm				
Imax (dB)	49.34±9.68	51.85±3.33	−0.982	0.336
Imean (dB)	12.61±4.87	15.67±2.95	−1.547	0.135

The data are expressed as mean ± standard deviation. CEUS, contrast-enhanced ultrasound; Imean, mean intensity; Imax, maximum intensity.

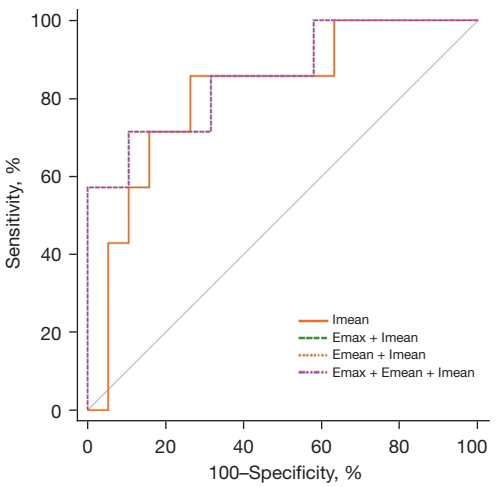

Figure 4 ROCs of the CEUS, and CEUS synchronized with SWE when shell was at 1.0 mm and AUC values for analyzing diagnostic performance. The AUC of Imean, Emax + Imean, Emean + Imean, Emax + Emean + Imean were 0.81 (95% CI: 0.61–0.94), 0.86 (95% CI: 0.67–0.96), 0.85 (95% CI: 0.66–0.96), 0.86 (95% CI: 0.67–0.96). ROC, receiver operating characteristic; CEUS, contrast-enhanced ultrasound; SWE, shear wave elastography; AUC, area under the curve; Emax, the maximum Young's moduli; Imean, the mean intensity; Emean, the mean Young's moduli; CI, confidence interval.

most cases. However, through this new real-time contrast elastography technique, we can obtain the elastic images that are as similar as possible to the images at peak intensity, which makes the quantitative parameters of elastic results and enhancement results more representative and more reliable. The result shows that the synchronization of SWE and CEUS of shell area had a larger AUC than that of the lesions. Emean + Imean and Emax + Emean + Imean of shell at 1.0 mm both had the highest AUC of 0.86 (95% CI: 0.67, 0.96), with a sensitivity and specificity of 71.43% and 89.47%, respectively, among all ROCs of SWE, CEUS, and SWE + CEUS (*Figure 4*). Although the sensitivities of SWE + CEUS were slightly reduced compared to CEUS alone, the specificities of SWE + CEUS were higher than those of CEUS. Therefore, quantitative analysis of the shell region of SWE + CEUS can effectively improve the diagnostic ability for breast lesions. For some BI-RADS 4 lesions that do not need clinical care, SWE + CEUS might circumvent unnecessary needle biopsies. For some malignant tumors, it is the optimal non-invasive tool for clinical diagnosis without postponing the appropriate therapy window.

Our research had some limitations. First, this was a single-center retrospective study with sampling bias, the

time period was brief, and there were only a few disease classifications. Second, depending on the operator's experience, the results of quantitative data could have been affected by the pressure exerted through the probe, and the radiologist could not outline the lesion precisely, resulting in the measurement of quantitative data being affected. Third, there was only one radiologist performing the examinations, the inter-observer variability was not considered, which could have impacted our results. Finally, we did not evaluate the diagnostic effectiveness of SWE and CEUS in combination with BI-RADS. Further studies with a large-scale, multicenter prospective study are needed to validate our results.

Conclusions

The peripheral enhancement of breast lesions is suggestive of malignancy, and the quantitative parameters of peripheral enhancement have a better diagnostic effect in discriminating benign and malignant breast lesions than the internal enhancement. Breast lesions can be more accurately diagnosed when SWE is synchronized with CEUS, which may give clinicians more information for clinical diagnosis and treatment.

Acknowledgments

Funding: This study was supported by the Natural Science Foundation of Zhejiang Province, China (No. LY20H180013).

Footnote

Reporting Checklist: The authors have completed the STARD reporting checklist. Available at https://gs.amegroups.com/article/view/10.21037/gs-22-684/rc

Data Sharing Statement: Available at https://gs.amegroups.com/article/view/10.21037/gs-22-684/dss

Conflicts of Interest: All authors have completed the ICMJE uniform disclosure form (available at https://gs.amegroups.com/article/view/10.21037/gs-22-684/coif). JP is from Shenzhen Mindray Bio-medical Electronics Co., Ltd. The other authors have no conflicts of interest to declare.

Ethical Statement: The authors are accountable for all aspects of the work in ensuring that questions related to the accuracy or integrity of any part of the work are appropriately investigated and resolved. The study was conducted in accordance with the Declaration of Helsinki (as revised in 2013). The study was approved by Ethics Committee of the Fourth Affiliated Hospital of Zhejiang University School of Medicine (No. K2022168) and individual consent for this retrospective analysis was waived.

References

1. Sung H, Ferlay J, Siegel RL, et al. Global Cancer Statistics 2020: GLOBOCAN Estimates of Incidence and Mortality Worldwide for 36 Cancers in 185 Countries. CA Cancer J Clin 2021;71:209-49.
2. Chen W, Zheng R, Baade PD, et al. Cancer statistics in China, 2015. CA Cancer J Clin 2016;66:115-32.
3. Cao W, Chen HD, Yu YW, et al. Changing profiles of cancer burden worldwide and in China: a secondary analysis of the global cancer statistics 2020. Chin Med J (Engl) 2021;134:783-91.
4. Jia WR, Chai WM, Tang L, et al. Three-dimensional contrast enhanced ultrasound score and dynamic contrast-enhanced magnetic resonance imaging score in evaluating breast tumor angiogenesis: correlation with biological factors. Eur J Radiol 2014;83:1098-105.
5. Lee EJ, Jung HK, Ko KH, et al. Diagnostic performances of shear wave elastography: which parameter to use in differential diagnosis of solid breast masses? Eur Radiol 2013;23:1803-11.
6. Xiao Y, Yu Y, Niu L, et al. Quantitative evaluation of peripheral tissue elasticity for ultrasound-detected breast lesions. Clin Radiol 2016;71:896-904.
7. Wang B, Chen YY, Yang S, et al. Combined Use of Shear Wave Elastography, Microvascular Doppler Ultrasound Technique, and BI-RADS for the Differentiation of Benign and Malignant Breast Masses. Front Oncol 2022;12:906501.
8. Cui YY, He NA, Ye XJ, et al. Evaluation of Tissue

Stiffness Around Lesions by Sound Touch Shear Wave Elastography in Breast Malignancy Diagnosis. Ultrasound Med Biol 2022;48:1672-80.
9. Park AY, Kwon M, Woo OH, et al. A Prospective Study on the Value of Ultrasound Microflow Assessment to Distinguish Malignant from Benign Solid Breast Masses: Association between Ultrasound Parameters and Histologic Microvessel Densities. Korean J Radiol 2019;20:759-72.
10. Giuseppetti GM, Baldassarre S, Marconi E. Color Doppler sonography. Eur J Radiol 1998;27 Suppl 2:S254-8.
11. Liu H, Jiang Y, Dai Q, et al. Peripheral enhancement of breast cancers on contrast-enhanced ultrasound: correlation with microvessel density and vascular endothelial growth factor expression. Ultrasound Med Biol 2014;40:293-9.
12. Raza S, Baum JK. Solid breast lesions: evaluation with power Doppler US. Radiology 1997;203:164-8.
13. Fang K, Wang L, Huang H, et al. Construction of Nucleolin-Targeted Lipid Nanobubbles and Contrast-Enhanced Ultrasound Molecular Imaging in Triple-Negative Breast Cancer. Pharm Res 2020;37:145.
14. Levental KR, Yu H, Kass L, et al. Matrix crosslinking forces tumor progression by enhancing integrin signaling. Cell 2009;139:891-906.
15. Xiang LH, Yao MH, Xu G, et al. Diagnostic value of contrast-enhanced ultrasound and shear-wave elastography for breast lesions of sub-centimeter. Clin Hemorheol Microcirc 2017;67:69-80.
16. Kapetas P, Clauser P, Woitek R, et al. Quantitative Multiparametric Breast Ultrasound: Application of Contrast-Enhanced Ultrasound and Elastography Leads to an Improved Differentiation of Benign and Malignant Lesions. Invest Radiol 2019;54:257-64.
17. Saracco A, Szabó BK, Aspelin P, et al. Contrast-enhanced ultrasound using real-time contrast harmonic imaging in invasive breast cancer: comparison of enhancement dynamics with three different doses of contrast agent. Acta Radiol 2015;56:34-41.
18. Choi HY, Seo M, Sohn YM, et al. Shear wave elastography for the diagnosis of small (≤2 cm) breast lesions: added value and factors associated with false results. Br J Radiol 2019;92:20180341.
19. Łukasiewicz E, Ziemiecka A, Jakubowski W, et al. Fine-needle versus core-needle biopsy - which one to choose in preoperative assessment of focal lesions in the breasts? Literature review. J Ultrason 2017;17:267-74.
20. Evans A, Whelehan P, Thomson K, et al. Quantitative shear wave ultrasound elastography: initial experience in solid breast masses. Breast Cancer Res 2010;12:R104.
21. Xie X, Zhang Q, Liu S, et al. Value of quantitative sound touch elastography of tissues around breast lesions in the evaluation of malignancy. Clin Radiol 2021;76:79.e21-8.
22. Huang L, Ma M, Du Z, et al. Quantitative evaluation of tissue stiffness around lesion by sound touch elastography in the diagnosis of benign and malignant breast lesions. PLoS One 2019;14:e0219943.
23. Yang H, Xu Y, Zhao Y, et al. The role of tissue elasticity in the differential diagnosis of benign and malignant breast lesions using shear wave elastography. BMC Cancer 2020;20:930.
24. Wang ZL, Sun L, Li Y, et al. Relationship between elasticity and collagen fiber content in breast disease: a preliminary report. Ultrasonics 2015;57:44-9.
25. Tozaki M, Fukuma E. Pattern classification of ShearWave™ Elastography images for differential diagnosis between benign and malignant solid breast masses. Acta Radiol 2011;52:1069-75.
26. Jiang T, Jiang Y, Chen W, et al. Chinese association of ultrasound in medicine and engineering, superficial organs and peripheral vessels committee expert consensus on clinical frequently asked questions in breast ultrasonography, June 2018. J Cancer Res Ther 2018;14:1463-8.
27. Li X, Li Y, Zhu Y, et al. Association between enhancement patterns and parameters of contrast-enhanced ultrasound and microvessel distribution in breast cancer. Oncol Lett 2018;15:5643-9.
28. Lee SH, Cho N, Kim SJ, et al. Correlation between high resolution dynamic MR features and prognostic factors in breast cancer. Korean J Radiol 2008;9:10-8.
29. Chang YW, Kwon KH, Choi DL, et al. Magnetic resonance imaging of breast cancer and correlation with prognostic factors. Acta Radiol 2009;50:990-8.
30. Liu H, Jiang YX, Liu JB, et al. Evaluation of breast lesions with contrast-enhanced ultrasound using the microvascular imaging technique: initial observations. Breast 2008;17:532-9.
31. Xu P, Wu M, Yang M, et al. Evaluation of internal and shell stiffness in the differential diagnosis of breast non-mass lesions by shear wave elastography. World J Clin Cases 2020;8:2510-9.
32. Lee EJ, Chang YW. Combination of Quantitative Parameters of Shear Wave Elastography and Superb Microvascular Imaging to Evaluate Breast Masses. Korean

J Radiol 2020;21:1045-54.
33. Ding Z, Liu W, He N, et al. Value of ultrasound elastography combined with contrast-enhanced ultrasound and micro-flow imaging in differential diagnosis of benign and malignant breast lesions. Am J Transl Res 2021;13:13941-9.

(English Language Editor: J. Jones)

Cite this article as: He H, Wu X, Jiang M, Xu Z, Zhang X, Pan J, Fu X, Luo Y, Chen J. Diagnostic accuracy of contrast-enhanced ultrasound synchronized with shear wave elastography in the differential diagnosis of benign and malignant breast lesions: a diagnostic test. Gland Surg 2023;12(1):54-66. doi: 10.21037/gs-22-684